Published in final edited form as:
Toxicol Appl Pharmacol. 2008 May 15; 229(1): 44–55. doi:10.1016/j.taap.2007.12.030.

Fullerene C_{60} exposure elicits an oxidative stress response in embryonic zebrafish

Crystal Y. Usenko, **Stacey L. Harper**, and **Robert L. Tanguay***
Department of Environmental and Molecular Toxicology and the Environmental Health Sciences Center, Oregon State University Corvallis, OR 97331

Abstract

Due to its unique physicochemical and optical properties, C_{60} has raised interest in commercialization for a variety of products. While several reports have determined this nanomaterial to act as a powerful antioxidant, many other studies have demonstrated a strong oxidative potential through photoactivation. To directly address the oxidative potential of C_{60}, the effects of light and chemical supplementation and depletion of glutathione (GSH) on C_{60}-induced toxicity were evaluated. Embryonic zebrafish were used as a model organism to examine the potential of C_{60} to elicit oxidative stress responses. Reduced light during C_{60} exposure significantly decreased mortality and the incidence of fin malformations and pericardial edema at 200 and 300 ppb C_{60}. Embryos co-exposed to the glutathione precursor, *N*-acetylcysteine (NAC), also showed reduced mortality and pericardial edema; however, fin malformations were not reduced. Conversely, co-exposure to the GSH synthesis inhibitors, butathionine sulfoximine (BSO) and diethyl maleate (DEM), increased the sensitivity of zebrafish to C_{60} exposure. Co-exposure of C_{60} or its hydroxylated derivative, $C_{60}(OH)_{24}$, with H_2O_2 resulted in increased mortality along the concentration gradient of H_2O_2 for both materials. Microarrays were used to examine the effects of C_{60} on the global gene expression at two time points, 36 and 48 hours post fertilization (hpf). At both life stages there were alterations in the expression of several key stress response genes including glutathione-*S*-transferase, glutamate cysteine ligase, ferritin, α-tocopherol transport protein and heat shock protein 70. These results support the hypothesis that C_{60} induces oxidative stress in this model system.

Keywords

fullerene; photoactivation; gene expression

Introduction

Carbon fullerenes, otherwise known as Buckminster fullerenes, or “bucky balls”, have unique physicochemical properties that may be exploited for use in consumer products such as cosmetics, lubricants, food supplements, building materials, clothing treatment, electronics and fuel cells (Loutfy *et al*., 2002). While fullerenes are currently produced by the ton every year, actual commercialization is still mostly under development (Robichaud *et al*., 2005). Due to

*Corresponding Author: Robert L. Tanguay, Ph.D., Department of Environmental and Molecular Toxicology, Environmental Health Sciences Center, Marine and Freshwater Biomedical Sciences Center, 1007 ALS, Oregon State University, Corvallis, OR 97331-7301, 541-737-6514 (voice), 541-737-7966 (fax) robert.tanguay@oregonstate.edu.

the potential for widespread applications and consequently, widespread exposures, evaluation of the biological effects of these important nanomaterials is warranted. C_{60} has been shown to induce toxicity in numerous cell culture and whole animal systems (Oberdorster, 2004; Sayes *et al.*, 2005; Isakovic *et al.*, 2006; Usenko *et al.*, 2007). However, contradictory reports in the literature make it difficult to interpret the mechanism by which C_{60} toxicity is induced.

Fullerene C_{60} has been described as a free radical scavenger by some (Dugan *et al.*, 1996; Wang *et al.*, 1999; Mori *et al.*, 2006) yet others have reported it to generate oxygen free radicals within and outside of biological systems (Yamakoshi *et al.*, 2003; Isakovic *et al.*, 2006). With few exceptions, pristine C_{60} and suspensions of C_{60} clusters (nC_{60}) are reportedly more toxic than their derivatives (Isakovic *et al.*, 2006). In cell culture, nC_{60} synergized the effects of oxidative stress-inducing agents and elicited cytotoxic action through cell membrane lipid peroxidation (Sayes *et al.*, 2005; Isakovic *et al.*, 2006). *In vivo*, nC_{60} induced oxidative stress and lipid peroxidation in the brain of juvenile largemouth bass (Oberdorster, 2004). However, others have reported C_{60} to act as a powerful antioxidant *in vivo* in rats with no acute or subacute toxicities (Gharbi *et al.*, 2005). Certain surface modifications (e.g. hydroxylation) have been shown to impart cytoprotective activity by eliminating reactive oxygen species (ROS) and antagonizing the effects of the oxidative stress-dependent cytotoxicity (Dugan *et al.*, 2001; Bogdanovic *et al.*, 2004; Isakovic *et al.*, 2006). In fact, carboxylated-C_{60} has been patented as a method to increase a metazoan's lifespan presumably through these same mechanisms (Dugan *et al.*, 2003). Despite disagreement amongst researchers as to the oxidative potential of C_{60}, oxidative stress is currently the leading proposed mechanism through which fullerenes may induce toxicity.

Oxidative stress is a common pathway of toxicity and disease. An organism can undergo oxidative stress through several different mechanisms. First, it may be directly induced by an oxidizing agent, such as H_2O_2. Second, it may be produced through the induction of cytochrome P450, as is the case with many polycyclic aromatic hydrocarbons (PAHs) (Wassenberg and Di Giulio, 2004). Third, a xenobiotic may inhibit the production of antioxidant molecules, such as glutathione (GSH), that function to maintain oxidative balance (Anderson, 1998). GSH is an endogenous tripeptide enzyme and known free radical scavenger, thus, it is important for detoxification of metabolites and ROS associated with chemical exposure and disease (Asikainen *et al.*, 2002; Franklin *et al.*, 2002; Suh *et al.*, 2004). It has yet to be determined through which, if any, of these pathways fullerenes may act.

The physicochemical properties of C_{60} support the hypothesis that this nanomaterial may induce oxidative stress following photoactivation. Due to its unique spherical structure, C_{60} has the ability to accept up to 6 electrons (Jensen *et al.*, 1996). These electrons essentially race around the structure through dipole moments. When C_{60} is acted upon by light, it is raised to a higher energy level producing singlet C_{60}, which reacts with O_2 to form singlet oxygen ($^1O_2$) (Hirsch and Brettreich, 2005). The amount of UV absorption necessary to raise the molecule to the triplet state varies with surface functionalization (Prat *et al.*, 1999). In general, more functional groups added to the fullerene requires more energy to move to the excited state, resulting in lower triplet and singlet oxygen quantum yields (Prat *et al.*, 1999). In the presence of C_{60}, both visible and ultraviolet light can generate ROS, particularly as singlet oxygen and superoxide (Pickering and Wiesner, 2005). These byproducts can induce oxidative stress leading to a variety of detrimental downstream effects such as lipid peroxidation, DNA and protein adduction and cellular death (Kamat *et al.*, 2000; Dugan *et al.*, 2001; Dhawan *et al.*, 2006).

In these studies, we exploit the numerous advantages of the embryonic zebrafish model to elucidate the mechanism by which C_{60} induces its toxic actions. This model has been used extensively for drug discovery and chemical or nanomaterial screening to rapidly evaluate

integrated system effects and subsequently identify mechanisms of toxic action (Usenko *et al.*, 2007). Here, we tested the effect of light activation and antioxidant environment on C_{60} toxic potential, and used zebrafish microarrays to evaluate global gene expression following C_{60} exposure. Further, we evaluated both C_{60} and hydroxylated C_{60} for antioxidative protection from H_2O_2 exposure. The results presented herein strongly indicate oxidative stress as a pathway of C_{60}-induced toxicity in this experimental model.

Methods

Solution Preparation

C_{60} was obtained from Sigma Aldrich, WI (99+%) and dissolved in 100% dimethyl sulfoxide (DMSO). The stock solution of 50 ppm C_{60} was sonicated for 1.5 hours to ensure a uniform dispersion and size distribution. $C_{60}(OH)_{24}$ (MER Corp, Arizona) was dissolved in DMSO and sonicated for 5 minutes to ensure uniform distribution. The size range of C_{60} and $C_{60}(OH)_{24}$ agglomerates following sonication were measured using photon correlation spectroscopy and previously reported in Usenko *et al.*, 2007. H_2O_2 was purchased from VWR International (Brisbane, CA) and was diluted to make exposure solutions of 0.5 mM and 1.0 mM. Buthionine sulfoximide (BSO), diethyl maleate (DEM), *N*-acetylcysteine (NAC), and L-glutathione (GSH) were purchased from Sigma Aldrich (St. Louis, MO).

General Exposure Protocol

Embryonic zebrafish were obtained from the AB strain of zebrafish (*Danio rerio*) reared in the Sinnhuber Aquatic Research Laboratory (SARL) at Oregon State University. Adults were kept at standard laboratory conditions of 28 °C on a 14 h light/10 h dark photoperiod with a conductivity of 500 Siemens per meter. Water consisted of reverse osmosis (RO) water supplemented with a commercially available salt solution (0.6% Instant Ocean®). Zebrafish were spawned and embryos were collected and staged (Reimers *et al.*, 2006). The chorion, an acellular envelope surrounding the embryo, was removed via enzymatic reaction with pronase at 24 hours post fertilization (hpf) as described previously (Usenko *et al.*, 2007). At 24 hpf, embryos were placed individually into wells of a 96-well plate, so that there was one embryo per well, and exposed to 100 μl of nanomaterial solution.. A 1% DMSO in water solution was used as a control as this concentration was previously found to have no effect on the embryos. Embryos were evaluated every 24 hours for 5 days for morphological malformations, mortality and behavioral abnormalities.

Dark Exposure

To determine if light influenced the toxic potential of C_{60}, the stock solution was prepared and kept in the dark and the 96-well plates were protected from the light after exposure. Embryos were dechorionated at 24 hpf and placed individually in wells and exposed to 1% DMSO controls, 100, 200, 300, or 500 ppb C_{60} (equivalent to 0, 0.05, 0.1, 0.15, 0.25 ng/mg as reported in Isaacson *et al*., 2007). Embryos were analyzed daily until 120 hpf for physiological malformations and mortality. The cumulative results were reported for effects. Sublethal effects were scored against number of surviving animals at the initial assessment (24 hours of exposure).

Co-incubation with GSH level-modifying Chemicals

The concentration-response of each of the test chemicals was conducted to determine the levels at which there was an adverse effect. Embryos were dechorionated at 24 hpf and were scored daily until 120 hpf. Embryos were co-incubated with either 100 μM GSH, 50 μM NAC, 250 μM ascorbic acid, 5 μM BSO, or 50 nM DEM. Previous reports found the maximum tolerable concentration (MTC) ascorbic acid to be 250 μM and GSH to be 100 μM (Hirsch and Brettreich,

2005). A concentration gradient was used for other co-incubations in this study. NAC is the rate-limiting substrate in GSH synthesis, and thus was used to potentially increase GSH production. BSO and DEM were used to inhibit GSH synthesis, thus making the embryos more sensitive to oxidative stressors. All chemicals were co-incubated with 50–300 ppb C_{60} or 1% DMSO and evaluated as described above. The pH of exposure solutions was monitored and buffered appropriately. H_2O_2 is a known oxidant and was co-incubated with 10 ppb C_{60} or 100 ppb $C_{60}(OH)_{24}$ to determine if either fullerene shifted the concentration-response curve to the right or left. H_2O_2 was co-incubated at 0.5 mM and 1.0 mM based on initial concentration-response of H_2O_2. At 1.0 mM, H_2O_2 induced 100% mortality.

Cellular Death Assays

Cellular death was evaluated in embryos co-exposed to C_{60} and NAC, DEM, BSO or ascorbic acid. This endpoint serves as an early indicator of perturbation based on previous evaluations that showed significant cell death could be detected after only 12 hours of exposure to C_{60} (Reimers *et al.*, 2006). Since cellular death was evaluated in whole embryos, potential targets of toxi city could be identified. Embryos were exposed to 100 ppb C_{60} or 1% DMSO and were co-exposed to 50 μM NAC, 50 nM DEM, 5 μM BSO, or 250μM ascorbic acid at 24 hpf. At 36 hpf, embryos were rinsed with water and then incubated in 100 μl of 5 μg/ml acridine orange for one hour in the dark at 28 °C. Embryos were rinsed again, mounted in low melt agarose (1% w/v, Promega, Madison, WI) and imaged using an Axiovert 200M Zeiss microscope (Carl Zeiss International, Germany) with a 546 nm filter. Fluorescence in the head region was measured and quantified using ImagePro Plus software (Media Cybernetics, Inc., Silver Spring, MD).

Global Gene Expression Analysis

Custom Array Chip—Oligonucleotides (50 mer) were purchased from MWG (High Point, NC). Zebrafish custom arrays of 14,000 genes were spotted by Eric Johnson at University of Oregon. Epoxy-coated slides were cross-linked and were kept at room temperature in a dessicator until use.

Isolation of RNA—Embryos were exposed to 200 ppb C_{60} or 1% DMSO at 24 hpf until 36 or 48 hpf and then pooled into three groups (biological replicates) of 40 embryos. Embryos were euthanized with tricaine methanesulfonate and rinsed thoroughly. Excess water was removed from the samples and 100 μl of TRIzol Reagent was added to extract RNA. Embryos were homogenized using a pestle on ice and stored at −80 °C until processing. Once all samples were collected, homogenates were thawed and 900 μl of TriReagent was added and each sample was vortexed. Next, the homogenates were centrifuged at 12,000 g at 4 °C, and then 200 μl chloroform was added. The samples were centrifuged again and the supernatants aliquoted into new vials. 500 μl of isopropanol was added to each sample and the sample was centrifuged. All liquid was removed and the pellet was washed several times with 70% ethanol: H_2O. The pellets were air dried and then resuspended in 30 μl diethylpyrocarbonate-water. The extractions were flash frozen using liquid nitrogen and stored at −80 °C. RNA was quantified using NanoDrop sensor and the quality verified using Agilent's BioAnalyzer 2100 (Palo Alto, CA) at the Center for Genome Research and Biocomputing (CGRB) at OSU.

Processing—Labeling, hybridization and scanning were performed at the CGRB. A Genisphere 950 labeling kit (Hatfield, PA) was the hybridization label for the samples. A dye swap for each sample was done to eliminate variability due to dye affinities. One microgram of RNA of each sample was reverse-transcribed with Superscript II (Invitrogen) using the Genisphere olido d(T) primer containing a capture sequence for the Cy3 or Cy5 labeling reagents. Slides were scanned using a GenePix Scanner at 543 nm for Cy3 and 633 for Cy5 at 80% power. Data was compiled using Gene Pix Software.

Data Analysis—Values from corresponding dye swaps were averaged between individual samples to obtain a single value for each sample. Treatments were conducted in triplicate for significance validation. Image files were quantified using QuantArray (PerkinElmer) and the raw data was imported into BASE software. Raw mean backgrounds were subtracted using LOWESS in order to eliminate dye-related artifacts. Genes induced or repressed by greater than 2-fold in all three replicates were selected and placed into categories based on function.

qPCR—Oxidative stress response genes were validated using quantitative real time polymerase chain reaction (qRT-PCR). cDNA was made from the RNA isolated for the microarrays. Briefly, cDNA was synthesized from 1 μg of total RNA per group using Superscript II (Life Technologies, Gaithersburg, MD) and oligo(dT) primers in a 20 ml volume. Primers were designed and ordered from MWG (High Point, NC) for several targeted genes (sequences given in table 1). Quantitative PCR was conducted using gene specific primers with the Opticon-2 real-time PCR detection system (MJ Research, Waltham, MA). For each PCR reaction, 1 μl of cDNA was used in the presence of SYBR Green, using DyNAmo SYBR green qPCR kit according to the manufacturer's instructions (Finnzymes, Espoo, Finland). A temperature gradient (54 °C–58 °C) was used to determine the appropriate annealing temperature for each primer set. All primers had an annealing temperature of 58 °C and ran for 35 cycles. The PCR product was separated using gel electrophoresis to ensure only one product was made. The PCR product was mixed with 6x SDS dye and loaded onto a 1.5% agarose gel with 0.05% ethidium bromide. The gel electrophoresis was run at 110 V and 80 mA for 1 hour. The gel was viewed on an Ultraviolet Transilluminator and imaged with a Polaroid photo documentation camera. PCR data was analyzed against an adult cDNA calibrator using the GAPDH primer set by the Opticon Monitor 3.1 software (MJ Research, Waltham, MA). Each sample PCR product was analyzed against a glyceraldehydes-3-phosphate dehydrogenase (GAPDH) control for that sample.

Statistical Analysis—All statistics were compiled using SigmaStat and plotted using Sigma Plot (SPSS Inc, Chicago, IL). Two-way analysis of variance (ANOVA) was used to detect significant differences between control and treated groups at a $p < 0.05$. All exposure studies had an $N = 24$ with 80% confidence interval. Significance was determined for cellular death assays using two-way ANOVA ($p < 0.05$), $N = 12$.

Results

Light activation of C_{60}

Oxidative stress was probed at the physical-chemical level since ROS generation by C_{60} has been shown to be photoactivated (Wang *et al.*, 1999). Although exposure in the dark was not completely protective, it did reduce the physiologic response of C_{60} exposure. There was a significant reduction in fin malformations, pericardial edema and mortality in the 200 and 300 ppb exposure groups when exposed in the dark (figure 1). Mortality was reduced by 30% at 200 and 300 ppb; however, 500 ppb C_{60} still induced 100% mortality within the first 24 hours of exposure (figure 1 A). Fin malformations were reduced by approximately 40% and pericardial edema was reduced by 85% at 200 ppb (figure 1 B, C). The presence or absence of light did not have an effect on development of the embryos.

Chemical supplementation of GSH and ascorbic acid

ROS-induced toxicity should be reduced by an increase in intracellular antioxidant levels. To determine if oxidative stress is a potential mechanism of C_{60}-induced responses, chemical alterations in GSH levels were evaluated. Co-incubation of 100 μM GSH with a concentration gradient of C_{60} did not alter the responses elicited by C_{60} alone (data not shown). Due to the low membrane permeability of GSH, embryos were co-exposed to NAC rather than GSH to

determine if favoring GSH synthesis would offer protection from C_{60}-induced responses. NAC can induce toxicity at high concentrations >300 μM (data not shown) so a low concentration (50 μM) was co-incubated with a concentration gradient of C_{60} (50–300 ppb C_{60}) (figure 2 A–C). NAC co-exposure with C_{60} reduced mortality by approximately 35% at 200 and 300 ppb and pericardial edema by 50% at 200 ppb C_{60} (figure 2 A,C). However, at concentrations of 300 ppb, the incidence of pericardial edema was significantly increased, most likely due to improved survival. NAC co-exposure to 1% DMSO did not have an effect compared to the 1% DMSO controls. Interestingly, co-exposure with NAC did not reduce the incidence of fin malformations at any concentration (figure 2 B).

An alternative approach to block ROS-induced toxicity is to increase intracellular antioxidant levels. Ascorbic acid (vitamin C) has been shown to protect zebrafish from ethanol-induced toxicity at 250 μM (Reimers *et al*., 2006). Embryos were co-exposed to 250 μM ascorbic acid and 50, 100, 200, and 300 ppb C_{60}. At 200 ppb C_{60}, there was a significant reduction in mortality; however at 300 ppb, 100% mortality was observed (figure 3 A). There was not a statistically significant difference between ascorbic acid controls (with 1% DMSO) and 1% DMSO controls. Unlike NAC, ascorbic acid reduced incidence of fin malformations at 200 ppb C_{60} (figure 3 B). At 200 ppb C_{60}, there was nearly complete protection from pericardial edema compared to background levels (figure 3 C).

Chemical depletion of GSH—BSO and DEM, known inhibitors of glutathione synthesis, were used to determine if C_{60} exerts a toxic response through depletion of glutathione. DEM was found to have a maximum tolerable concentration (MTC) of 50 nM and BSO had a MTC of 5 μM. These concentrations of DEM and BSO were used for each co-incubation with graded concentrations of C_{60} (50–300 ppb) and 1% DMSO controls. Both DEM and BSO increased the embryo's sensitivity to C_{60}, with increased mortality within the first 24 hours of exposure (figure 4). Embryos were more sensitive to DEM than BSO. There was not a significant increase in mortality between controls for either DEM or BSO and control embryos.

To more closely examine the C_{60}-elicited physiologic response following exposure to NAC or DEM, cellular death was evaluated in whole embryos. Embryos were co-incubated with 100 ppb C_{60} and 50 nM DEM, 5 μM BSO, 250 μM ascorbic acid or 100 μM NAC. Control embryos were incubated with 1% DMSO, and chemical controls were also co-incubated with 1% DMSO. DEM, BSO, and NAC did not induce cellular death when co-incubated with 1% DMSO. However, DEM and BSO significantly increased cell death when co-exposed to C_{60} compared to C_{60} exposed embryos (figure 5). NAC exposure offered only partially protected the embryo from C_{60}-induced cellular death. Ascorbic acid had no effect on cell death despite its protection from physiologic responses (data not shown).

Antioxidative Potential of Fullerenes—A study by Wang *et al.* (1999) found C_{60} to be a powerful antioxidant, even more powerful than vitamin E. So far, high levels of C_{60} have been investigated for oxidative potential; however, antioxidant properties may be observed only at very low concentrations. Low concentrations of C_{60} and $C_{60}(OH)_{24}$ (10 ppb and 500 ppb, respectively) were co-incubated with two concentrations of H_2O_2 (500 μM and 1 mM) to determine if C_{60} offered protection from H_2O_2-induced oxidative stress and mortality. These fullerene concentrations were previously reported to be 10-fold below the no observable adverse effect level (NOAEL) (Kamat *et al*., 1998; Kamat *et al.*, 2000). Neither co-exposure offered embryonic protection, but instead significantly increased mortality compared to embryos exposed only to H_2O_2 (figure 6).

Global Gene Expression—Custom zebrafish microarrays were used to identify the early genomic responses to C_{60} exposure. The microarray data was analyzed to determine the transcripts that were mis-regulated by more than 2 fold following exposure. Of the 234 and 95

genes that were up-regulated by C_{60} exposure at 36 hpf and 48 hpf, respectively, 66 genes were up-regulated at both time points. Only 15 genes were commonly down-regulated between the two time points. Genes were grouped by function and time of exposure (figure 7 A–D). Noteworthy, 24% and 19% of genes up-regulated at 36 and 48 hpf, respectively, were associated with a response to stress. These genes include GST-pi, GCLc, heat shock proteins and ferritin. Furthermore, there was up-regulation of development, cell cycle (including induction of apoptosis), signal transduction, and cytoskeleton and cytoplasmic transfer genes (figure 7). Examples of regulated genes from each category are given in table 2. See supporting information for complete list of genes. It is important to point out that for several of the genes the MWG oligo set contained multiple oligos for each target gene covering different regions of the transcript, and we found very little variation in intensity across array elements which further increased the confidence of the raw array data.

PCR—Five target genes that were found to be differentially expressed by microarray analysis were validated using qPCR: GST-pi, GCLc, ferritin heavy chain, α-tocopherol transport protein (TTP), and heat shock protein 70kD (HSP70). All genes chosen were significantly up-regulated over 2-fold. GAPDH was used as a loading control and adult zebrafish cDNA was used as a calibrator. These stress response genes were significantly up-regulated (figure 8). The abundance of GCLc was very low, resulting in a large fold induction. GST-pi had strong results with similar fold induction at both 36 and 48 hpf (figure 8 A). The results from PCR validated the directional regulation observed in the microarray analyses.

Discussion

In vivo evaluations conducted using embryonic zebrafish provide strong evidence indicating C_{60} is a powerful oxidant in the absence of functionalization. Four lines of evidence presented herein point to oxidative stress as a primary pathway of C_{60}-induced toxicity. First, physiologic responses and cellular death were inhibited by the absence of light during solution preparation and throughout the exposure period. A reduction in light resulted in reduced mortality and malformations, except at the highest concentration. While photoactivation strongly indicates oxidative stress as a mechanism of action, the lack of complete protection when exposed in the dark indicates this may not be the only mechanism of action. Lee *et al.* (2007) recently found that agglomeration size of C_{60} affects the degree to which C_{60} is able to mediate energy and electron transfer (Lee *et al.*, 2007). The large agglomeration sizes previously measured in our system indicate there could be a decrease in photoirradiation potential of C_{60} at higher concentrations (Kamat *et al.*, 2000; Yamakoshi *et al.*, 2003). Kamat and others demonstrated that when photoexcited, both C_{60} and hydroxylated C_{60} can induce membrane damage in rat hepatic and tumor microsomes by generation of ROS in a time- and concentration-dependent manner (Prat *et al.*, 1999). Although these photoactivation characteristics may be undesirable for healthy cells, this activity could be exploited for applications in biomedical science (Zhu *et al.*, 2007). For example, targeted drug delivery to tumors may be achieved via encapsulation of chemotherapeutics in C_{60} particles and subsequent illumination localized at the target site to activate C_{60} and trigger release of the drug. Additionally, surface groups could be used to alter the photochemical properties of fullerenes since they are apparently less responsive to light with increased functionalization (Kamat *et al.*, 1998; Sayes *et al.*, 2005).

A second line of evidence is provided by the change in sensitivity of embryonic zebrafish to C_{60} exposure that resulted from altered levels of the antioxidants GSH and ascorbic acid. Although administration of GSH itself did not have an effect on embryonic susceptibility, uptake of GSH into cells is thought to be limited requiring ATP for transport (Wang *et al.*, 1999). However, another study using embryonic zebrafish revealed that GSH co-exposure with tetrahydrofuran-C_{60} (THF-C_{60}) increased survival when compared to THF-C_{60} alone (Bogdanovic *et al.*, 2004). In this case, it may be that solubilization of C_{60} with THF changed

its physicochemical properties such that GSH interacted directly with THF-C_{60} in the exposure solution and reduced C_{60} uptake. Internal levels of GSH would need to be measured before and after waterborne GSH exposure to determine its uptake into biological systems.

Uptake limitations and uncertainties of GSH were overcome by using chemical that could deplete internal antioxidant pools. Depletion of antioxidants is one pathway through which nanomaterials could induce oxidative toxicity. When DEM and BSO were used to chemically inhibit glutathione production in embryonic zebrafish, the concentration-response curve shifted to the left; that is, a lower concentration of C_{60} was required to induce the same effects observed at higher concentrations. This not only implicates oxidative stress as a mechanism of C_{60} toxicity but also the highlights the importance of GSH in mediating the response. While DEM and BSO potentiated the effects of C_{60}, the addition of NAC offered protection from C_{60}-induced toxicity. NAC had been used in previous studies to increase GSH levels and protect organisms from oxidative stress (Kamat *et al*., 1998; Sayes *et al*., 2005). Similarly, our results demonstrated a significant reduction in mortality and pericardial edema in NAC co-incubated embryos. Fin malformations, however, were still present in all embryos exposed to concentrations of 200 ppb and 300 ppb. Co-exposure of embryos to C_{60} and ascorbic acid resulted in a significant reduction in mortality, pericardial edema and fin malformations, though at 300 ppb C_{60}, vitamin C could no longer provide protection and 100% of the embryos died. Our results concur with previous studies that found ascorbic acid to protect against C_{60}-induced cell death and lipid peroxidation. Collectively, these results suggest C_{60} has oxidative potential since depletion of antioxidants increased the sensitivity of zebrafish embryos to C_{60} exposure while antioxidant enhancement decreased their sensitivity.

The lack of antioxidative function observed from both C_{60} and $C_{60}(OH)_{24}$ when co-exposed with H_2O_2 provides the third line of evidence supporting an oxidative stress echanism of toxic action. Cell culture evaluations suggest that C_{60} acts as a stronger antioxidant than vitamin E, protecting against 1 mM H_2O_2. Derivatives of C_{60} have also been shown to exhibit antioxidant properties in numerous cell culture and whole animal studies (Sayes *et al.*, 2004; Kamat *et al.*, 1998; Yamakoshi *et al*., 2003; Sayes *et al*., 2005). Despite previous reports of antioxidant capabilities, neither C_{60} nor $C_{60}(OH)_{24}$ demonstrated antioxidant properties in the embryonic zebrafish model. In fact, rather than offering protection from H_2O_2 exposure, both C_{60} and its hydroxylated derivative significantly increased the deleterious oxidative effects. Delineation of those that possess antioxidant potential and those that do not should be addressed systematically since ‘fullerenes’ are already being marketed to consumers as antioxidants in cosmetics and night creams. Additionally, identification of fullerenes with antioxidant potential could be developed as therapeutic applications for central nervous system neurodegenerative diseases (i.e. Parkinson’s disease, Alzheimer’s disease, multiple sclerosis, amyotrophic lateral sclerosis, or Huntington’s disease), stroke, atherosclerosis, myocardial ischemia, myocardial reperfusion, diabetes, complications of diabetes, circulatory impairment, retinopathy, blindness, kidney disease, pancreas disease, neuropathy, gum disease, cataracts, skin disease, skin damage, radiation damage, damage caused by tobacco use, excessive angiogenesis, insufficient angiogenesis, hearing loss, collateral damage of chemotherapy, mucositis, senescence, hemorrhagic shock, distributive shock, septic shock, heat stroke, severe burn shock, or non-hemorrhagic trauma shock (Hartnagel *et al.*, 2006).

A final line of evidence indicates an oxidative stress mechanism of C_{60} toxicity. A zebrafish microarray developed from commercially available oligonucleotides was used to determine important genes and pathways that play a role in the response to C_{60} exposure. By analyzing two early time points during development, we were able to identify impacts that persist over multiple stages of development. Many of the genes known to be involved in an oxidative stress response were upregulated in embryonic zebrafish after exposure to C_{60}. In particular, two genes that were significantly up-regulated are directly related to glutathione activity: GST-*pi*

and GCLc. GCL is important for increasing GSH levels during oxidative stress, while GST is involved in the phase II metabolism conjugation of GSH to electrophilic xenobiotics. A study by Henry *et al*. also found GST-*pi* to be up-regulated; however, they attributed the up-regulation to the THF vehicle (Henry *et al.*, 2007). In our study, 1% DMSO was used as the vehicle, not THF, so the common alterations in gene expression were likely due to the C_{60} and not the solvent vehicle.

Microarray results revealed increased expression of additional oxidative stress-responsive genes. An increase in α-tocopherol transfer proteins (TTP) transcript levels further implicates an oxidative stress response and is in accordance with the previous studies which found α-tocopherol protected cells in culture from C_{60}-induced injury (Kamat *et al.*, 1998; Sayes *et al.*, 2005). Ferritin is a critical protein in detoxifying oxidative stress that has been linked to an antioxidant response element (ARE) (Iwasaki *et al.*, 2006). Up-regulation of ferritin in response to C_{60} exposure indicates a disruption in iron homeostasis and/or oxidative stress. Ferritin is regulated by levels of iron, cytokines, hormones and oxidative stress (Zandman-Goddard and Shoenfeld, 2007). There is a chance that C_{60} had direct effects on these factors and subsequent indirect effects on ferritin transcription; however, it is more likely that ferritin was up-regulated to bind iron and prevent propagation of the oxidative stress cascade. The role of iron and ferritin for oxidative stress responses is an important area of research, particularly with regards to their interbalance following a stroke and in neurodegenerative disorders such as Alzheimer's disease (Quitana *et al.*, 2006).

Disparity among reports on C_{60} oxidative potential could be attributed to the wide range of methods for solution preparation which likely have an impact on the biological activity and toxic potential of fullerenes. Our experimental design called for sonication of C_{60} in 100% DMSO with dilution to final exposure concentrations of 1% DMSO. Granted, the use of such a solvent would increase potential uptake but we were interested in specifically detailing the interactions of fullerenes within biological systems, not assessing uptake from the environment into the system. Other methods of solubilization include the use of THF, ethanol, methanol or stirring for prolonged periods in direct sunlight (Yamago *et al.*, 1995; Oberdorster, 2004; Sayes *et al.*, 2004; Dhawan *et al.*, 2006; Levi *et al.*, 2006; Lovern and Klaper, 2006; Zhu *et al.*, 2006). It is important to recognize that extensive methods of solubilization may also alter the physicochemical properties of C_{60}, thereby altering the interaction within the biological system. For example, with increased hydroxylation, the photosensitivity of C_{60} decreases. This could be of potential concern for protocols that require prolonged stirring of C_{60} in direct sunlight.

Results presented herein are in agreement with the studies that show C_{60} can act as a pro-oxidant and elicit a toxic response via oxidative stress (Kamat *et al.*, 1998; Yamakoshi *et al.*, 2003; Oberdorster, 2004; Sayes *et al.*, 2005). Chemically increasing antioxidant levels *in vivo* reduced adverse effects, while chemically inhibiting glutathione production increased sensitivity to C_{60} exposure. Functionalization of C_{60} may alter the biological response; however, there was no indication in this study to suggest that hydroxylation of C_{60} imparts antioxidant properties. Future studies should be focused on the role surface functionalization and methods of C_{60} preparation have on oxidative potential. The embryonic zebrafish has once again proven to be a valuable model for studying nanomaterial-biological interactions at multiple levels of biological organization, i.e. whole animal, cellular and molecular.

Acknowledgements

The authors would like to thank Eric Johnson and Jason Carriere for their assistance with the microarray slide preparation and hybridization protocol. We would also like to thank Caprice Rosato the Center for Gene Research and Biocomputing and Abby Benninghoff for assistance with microarray hybridization and data analysis. We would also like to acknowledge Jane LaDu for technical assistance. These studies were partially supported by the Oregon State

University Research Office, the Safer Nanomaterials and Nanomanufacturing Initiative of the Oregon Nanoscience and Microtechnologies Institute, EPA STAR grant RD-833320 and NIEHS grants ES03850 and ES07060.

References

Anderson ME. Glutathione: an overview of biosynthesis and modulation. Chem Biol Interact 1998;111–112:1–14.

Asikainen TM, Huang TT, Taskinen E, Levonen AL, Carlson E, Lapatto R, Epstein CJ, Raivio KO. Increased sensitivity of homozygous Sod2 mutant mice to oxygen toxicity. Free Radic Biol Med 2002;32:175–186. [PubMed: 11796207]

Bogdanovic G, Kojic V, Dordevic A, Canadanovic-Brunet J, Vojinovic-Miloradov M, Baltic VV. Modulating activity of fullerol C-60(OH)(22) on doxorubicin-induced cytotoxicity. Toxicol in Vitro 2004;18:629–637. [PubMed: 15251181]

Dhawan A, Taurozzi JS, Pandey AK, Shan WQ, Miller SM, Hashsham SA, Tarabara VV. Stable colloidal dispersions of C-60 fullerenes in water: Evidence for genotoxicity. Environmental Science & Technology 2006;40:7394–7401. [PubMed: 17180994]

Dugan LL, Lovett E, Quick K, Hardt J. Carboxylated C60 increases metazoan lifespan (United States). 2003

Dugan LL, Gabrielesen JK, Yu SP, Lin TS, Choi DW. Buckminsterfullerenol free radical scavengers reduce excitotoxic and apoptotic death of cultured cortical neurons. Neurobiology of Disease 1996;3:129–135. [PubMed: 9173920]

Dugan LL, Lovett EG, Quick KL, Lotharius J, Lin TT, O'Malley KL. Fullerene-based antioxidants and neurodegenerative disorders. Parkinsonism Relat D 2001;7:243–246.

Franklin CC, Krejsa CM, Pierce RH, White CC, Fausto N, Kavanagh TJ. Caspase-3-dependent cleavage of the glutamate-L-cysteine ligase catalytic subunit during apoptotic cell death. American Journal of Pathology 2002;160:1887–1894. [PubMed: 12000740]

Gharbi N, Pressac M, Hadchouel M, Szwarc H, Wilson SR, Moussa F. [60]fullerene is a powerful antioxidant in vivo with no acute or subacute toxicity. Nano Lett 2005;5:2578–2585. [PubMed: 16351219]

Hartnagel U, Erlangen D, Hirsch A, Lebovitz R. fullerene compositions and their use as antioxidants (United States). 2006

Henry TB, Menn FM, Fleming JT, Wilgus J, Compton RN, Sayler GS. Attributing effects of aqueous C60 nano-aggregates to tetrahydrofuran decomposition products in larval zebrafish by assessment of gene expression. Environ Health Perspect. 2007in press

Hirsch, A.; Brettreich, M. Fullerenes: chemistry and reactions. Weinheim: Wiley-VCH; 2005.

Isaacson CW, Usenko CY, Tanguay RL, Field JA. Quantification of fullerenes by LC/ESI-MS and its application to *in vivo* toxicity assays. Anal Chem 2007;79:9091–9097. [PubMed: 17963360]

Isakovic A, Markovic Z, Todorovic-Markovic B, Nikolic N, Vranjes-Djuric S, Mirkovic M, Dramicanin M, Harhaji L, Raicevic N, Nikolic Z, Trajkovic V. Distinct cytotoxic mechanisms of pristine versus hydroxylated fullerene. Toxicological Sciences 2006;91:173–183. [PubMed: 16476688]

Iwasaki K, Mackenzie EL, Hailemariam K, Sakamoto K, Tsuji Y. Hemin-mediated regulation of an antioxidant-responsive element of the human ferritin H gene and role of Ref-1 during erythroid differentiation of K562 cells. Mol Cell Biol 2006;26:2845–2856. [PubMed: 16537925]

Jensen AW, Wilson SR, Schuster DI. Biological applications of fullerenes. Bioorgan Med Chem 1996;4:767–779.

Kamat JP, Devasagayam TPA, Priyadarsini KI, Mohan H. Reactive oxygen species mediated membrane damage induced by fullerene derivatives and its possible biological implications. Toxicology 2000;155:55–61. [PubMed: 11154797]

Kamat JP, Devasagayam TPA, Priyadarsini KI, Mohan H, Mittal JP. Oxidative damage induced by the fullerene C-60 on photosensitization in rat liver microsomes. Chem-Biol Interact 1998;114:145–159. [PubMed: 9839628]

Kimmel C, Ballard W, Kimmel S, Ullmann B, Schilling T. Stages of embryonic development of the zebrafish. Developmental Dynamics 1995;203:253–310. [PubMed: 8589427]

Lee J, Fortner JD, Hughes JB, Kim JH. Photochemical production of reactive oxygen species by C_{60} in the aqueous phase duirng UV irradiation. Environmental Science & Technology 2007;41:2529–2535. [PubMed: 17438811]

Levi N, Hantgan RR, Lively MO, Carroll DL, Prasad GL. C60-Fullerenes: detection of intracellular photoluminescence and lack of cytotoxic effects. Journal of Nanobiotechnology 2006;4:14–25. [PubMed: 17169152]

Loutfy, RO.; Lowe, TP.; Moravsky, AP.; Katagiri, S. Perspectives of fullerene nanotechnology. Netherlands: Springer; 2002. Commercial production of fullerenes and carbon nanotubes; p. 35-46.

Lovern SB, Klaper R. *Daphnia magna* mortality when exposed to titanium dioxide and fullerene (C_{60}) nanoparticles. Environmental Toxicology & Chemistry 2006;25:1132–1137. [PubMed: 16629153]

Mori T, Takada H, Ito S, Matsubayashi K, Miwa N, Sawaguchi T. Preclinical studies on safety of fullerene upon acute oral administration and evaluation for no mutagenesis. Toxicology 2006;225:48–54. [PubMed: 16782258]

Oberdorster E. Manufactured nanomaterials (fullerenes, C_{60}) induce oxidative stress in the brain of juvenile largemouth bass. Environmental Health Prospectives 2004;112:1058–1062.

Pickering KD, Wiesner MR. Fullerol-sensitized production of reactive oxygen species in aqueous solution. Environmental Science & Technology 2005;39:1359–1365. [PubMed: 15787378]

Prat F, Stackow R, Bernstein R, Qian WY, Rubin Y, Foote CS. Triplet-state properties and singlet oxygen generation in a homologous series of functionalized fullerene derivatives. J Phys Chem A 1999;103:7230–7235.

Quitana C, Bellefqih S, Laval JY, Guerquin-Kern JL, Wu TD, Avila J, Ferrer I, Arranz R, Patino C. Study of the localization of iron, ferritin, and hemosiderin in Alzheimer's disease hippocampus by analytical microscopy at the subcellular level. J Struct Biol 2006:153.

Reimers MJ, La Du JK, Periera CB, Giovanini J, Tanguay RL. Ethanol-dependent toxicity in zebrafish is partially attenuated by antioxidants. Neurotoxicol Teratol 2006;28:497–508. [PubMed: 16904866]

Robichaud CL, Tanzil D, Weilenmann U, Wiesner MR. Relative risk analysis of several manufactured nanomaterials: an insurance industry context. Environ Sci Technol 2005;39:8985–8994. [PubMed: 16323804]

Sayes CM, Gobin AM, Ausman KD, Mendez J, West JL, Colvin VL. Nano-C60 cytotoxicity is due to lipid peroxidation. Biomaterials 2005;26:7587–7595. [PubMed: 16005959]

Sayes CM, Fortner JD, Guo W, Lyon D, Boyd AM, Ausman KD, Tao Y, Sitharaman B, Wilson L, Hughes J, West J, Colvin V. The differential cytotoxicity of water-soluble fullerenes. Nano Lett 2004;4:1881–1887.

Suh JH, Shenvi SV, Dixon BM, Liu H, Jaiswal AK, Liu RM, Hagen TM. Decline in transcriptional activity of Nrf2 causes age-related loss of glutathione synthesis, which is reversible with lipoic acid. Proc Natl Acad Sci U S A 2004;101:3381–3386. [PubMed: 14985508]

Usenko CY, Harper SL, Tanguay RL. *In vivo* evaluation of carbon fullerene toxicity using embryonic zebrafish. Carbon. 2007in press

Wang IC, Tai LA, Lee DD, Kanakamma PP, Shen CKF, Luh TY, Cheng CH, Hwang KC. C-60 and water-soluble fullerene derivatives as antioxidants against radical-initiated lipid peroxidation. Journal of Medicinal Chemistry 1999;42:4614–4620. [PubMed: 10579823]

Wassenberg DM, Di Giulio RT. Synergistic embryotoxicity of polycyclic aromatic hydrocarbon aryl hydrocarbon receptor Agonists with cytochrome P4501A inhibitors in Fundulus heteroclitus. Environ Health Persp 2004;112:1658–1664.

Yamago S, Tokuyama H, Nakamura E, Kikuchi K, Kananishi S, Sioelo L, Nakahara J, Enomoto S, Ambe F. In vivo biological behavior of a water-miscible fullerene: ^{14}C lableing, absorption, distribution, excretion and acute toxicity. Chemical Biology 1995;2:385–389.

Yamakoshi Y, Umezawa N, Ryu A, Arakane K, Miyata N, Goda Y, Masumizu T, Nagano T. Active oxygen species generated from photoexcited fullerene (C60) as potential medicines: O2-* versus 1O2. J Am Chem Soc 2003;125:12803–12809. [PubMed: 14558828]

Zandman-Goddard G, Shoenfeld Y. Ferritin in autoimmune diseases. Autoimmune Rev 2007;6:457–463.

Zhu S, Oberdorster E, Haasch ML. Toxicity of an engineered nanoparticle (fullerene, C60) in two aquatic species, Daphnia and fathead minnow. Mar Environ Res 2006;62(Suppl):S5–9. [PubMed: 16709433]

Zhu X, Zhu L, Li Y, Duan Z, Chen W, Alvarez PJJ. Developmental toxicity in zebrafish (*Danio Rerio*) embryos after exposure to manufactured nanomaterials: buckminsterfullerene aggregates (nC60) and fullerol. Environmental and Toxicological Chemistry 2007;26:976–979.

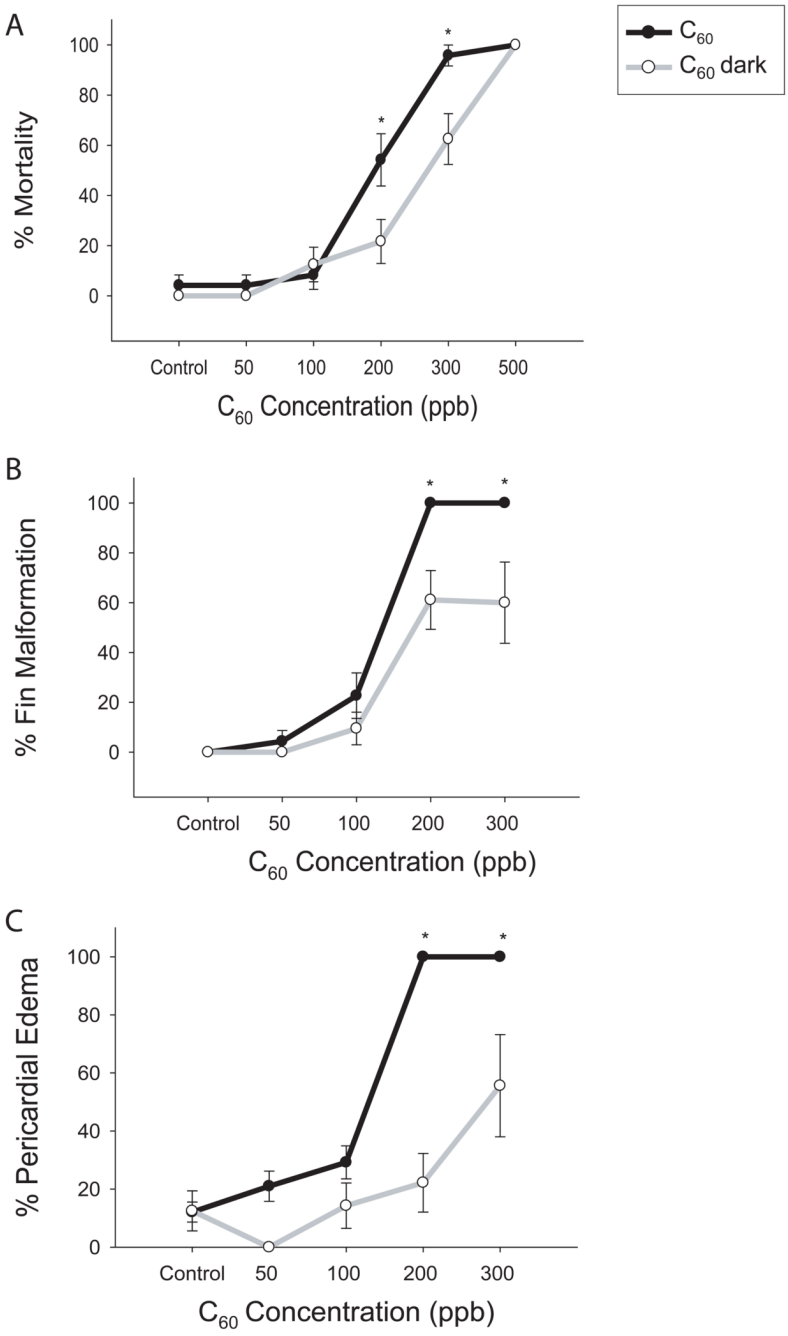

Figure 1. C_{60} concentration-response: dark vs. light exposure

24 hpf embryos were dechorionated and exposed in the dark to graded concentrations of C_{60}. Mortality (A), fin malformations (B), and pericardial edema (C) were scored daily for 5 days post exposure. Significant difference was determined using two-way ANOVA (*$p < 0.05$), N = 24, compared to C_{60} effect in the light at that concentration. Error bars represent the standard error of means (SEM).

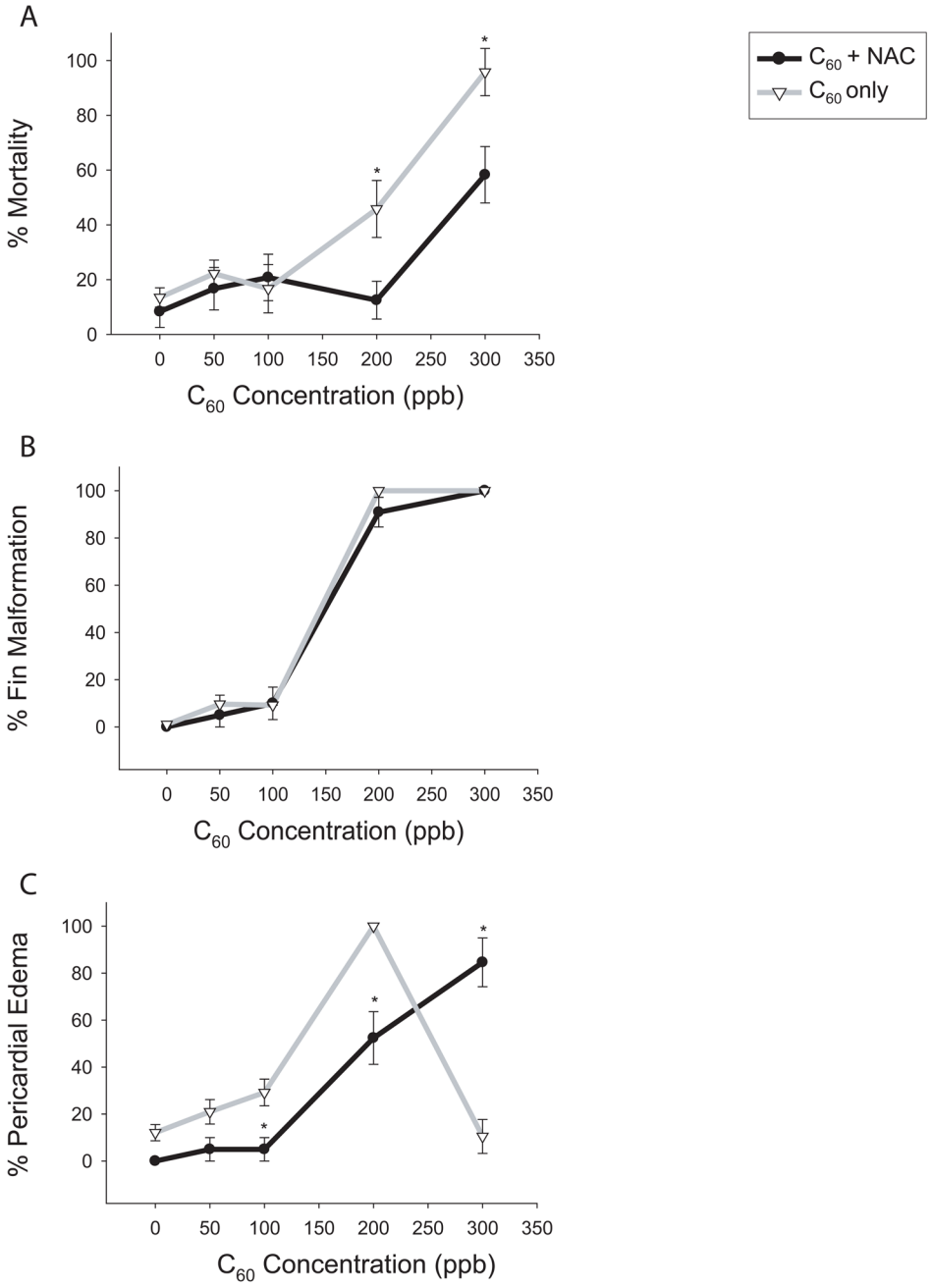

Figure 2. NAC co-incubation with C_{60}

Embryonic zebrafish were co-incubated with 50 μM NAC and graded concentrations of C_{60} from 24 to 120 hpf. (A) Cumulative mortality by 120 hpf for C_{60} + NAC (●) and C_{60} only (▽). (B) Percentage of embryos with fin malformation including those that died prior to 120 hpf. (C) Percentage of embryos with pericardial edema including those later scored for mortality. Significance was determined using two-way ANOVA, (*$p < 0.05$, $N = 24$), and error bars represent the +/− the SEM.

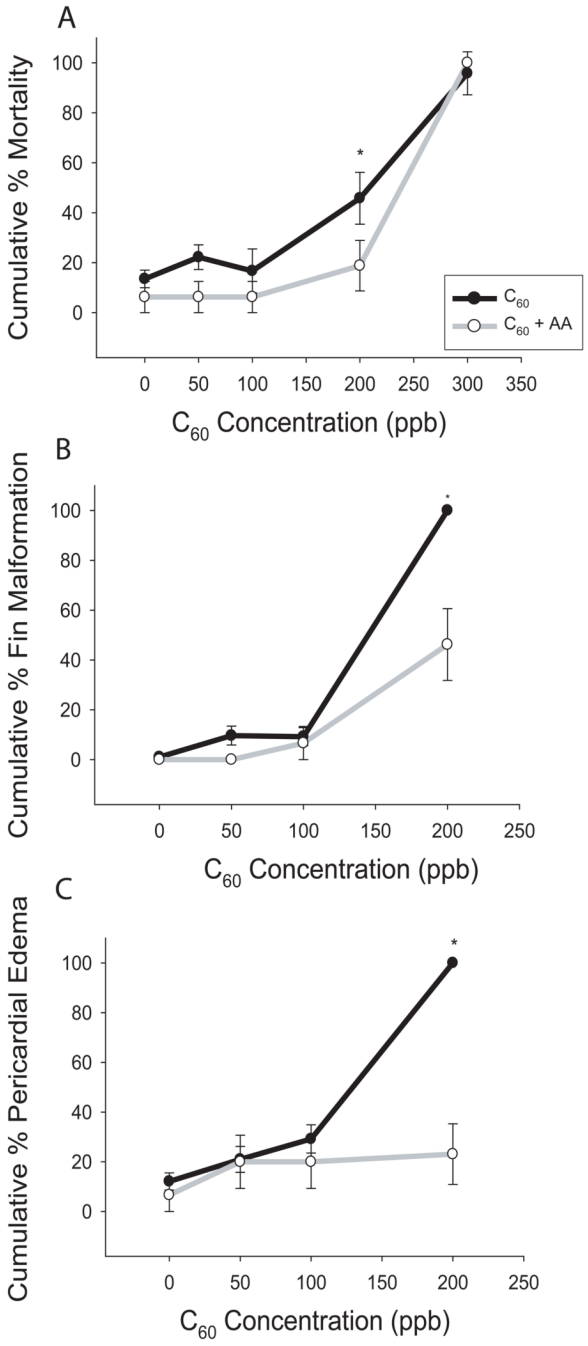

Figure 3. C_{60} co-incubation with ascorbic acid

Embryos were co-exposed to 250 μM ascorbic acid (AA) and graded concentrations of C_{60} at 24 hpf until 120 hpf. Ascorbic acid decreased (A) mortality, (B) fin malformations (FM), and (C) pericardial edema (PE) at 200 ppb C_{60}. Significance was determined by two-way ANOVA (*$p < 0.05$, N = 24), and error bars represent +/− the SEM.

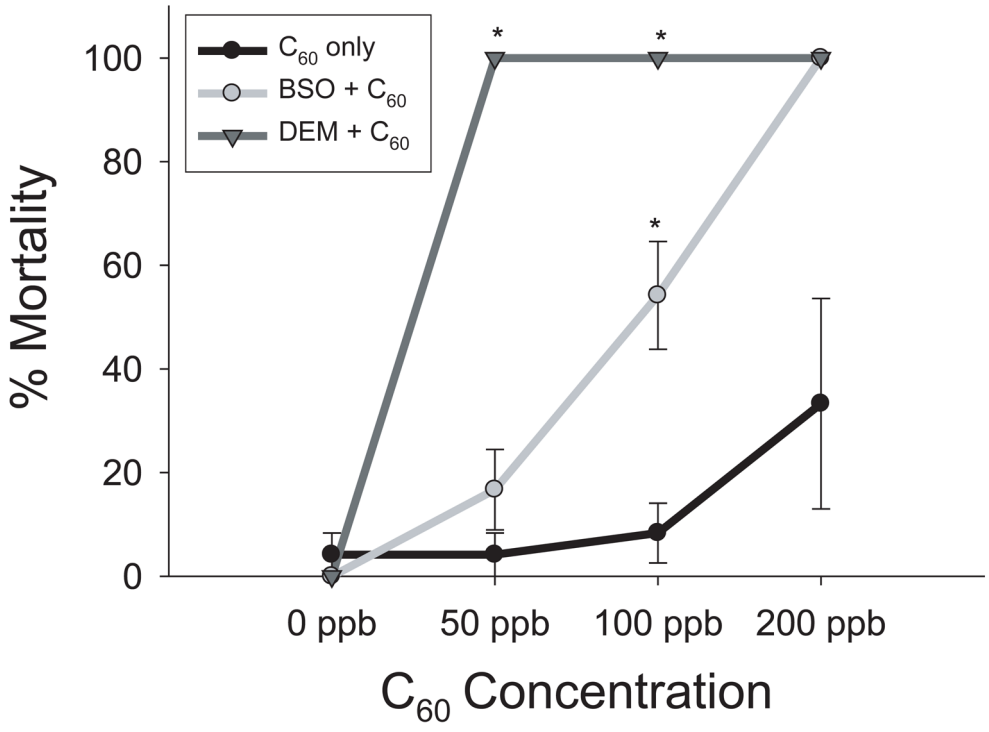

Figure 4. DEM and BSO concentration response

DEM and BSO were used to block glutathione production. Embryos were co-exposed to 5 μM BSO or 50 nM DEM and graded concentrations of C_{60} at 24 hpf for 24 hours. DEM shifted the LC_{50} to 50 ppb rather than 200 ppb. BSO induced 100% mortality at 200 ppb, but no significant mortality at 100 ppb. Significance was determined using two-way ANOVA (*$p < 0.05$, $N = 24$). Error bars represent +/− the SEM.

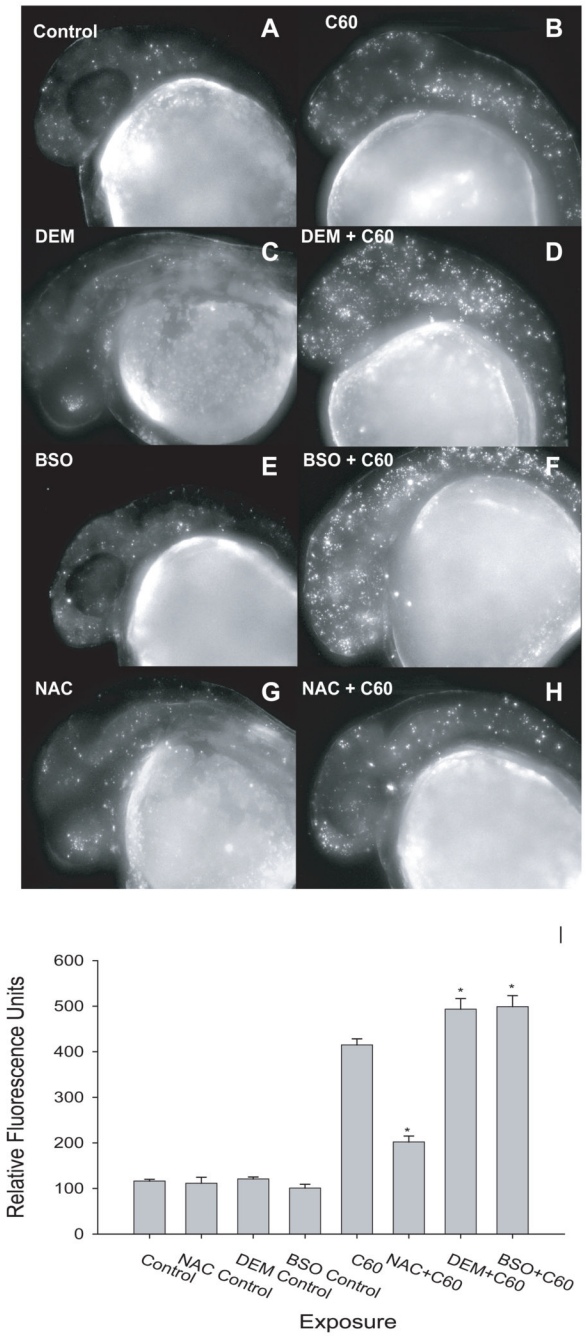

Figure 5. Cell death in co-exposures

Cell death was measured as a result of co-incubation with either NAC or DEM and 100 ppb C_{60}. Embryos were exposed at 24 hpf and cellular death was determined at 36 hpf using acridine orange. There was not a statistically significant difference between (A) control and (C) DEM, (E) BSO, or (G) NAC only. (D,E) DEM and BSO co-incubated with C_{60} significantly increased cell death compared to (B) C_{60} only. (H) NAC decreased cell death compared to C_{60} alone; however cell death was significantly higher than controls. Significance was determined using two-way ANOVA (*$p < 0.05$, $N = 12$).

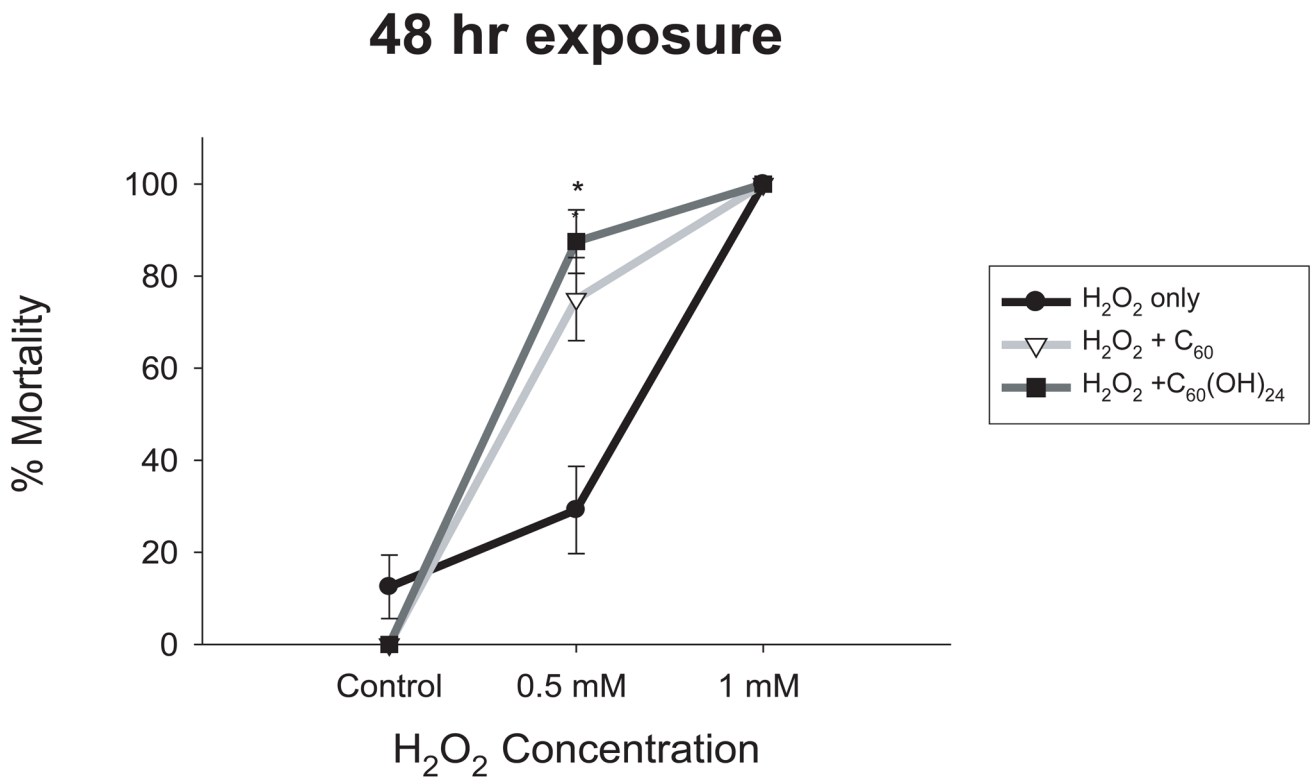

Figure 6. H_2O_2 and C_{60} co-incubation

Embryos were exposed to H_2O_2 at 24 hpf for 48 hours to determine the concentration-response. Embryos were co-exposed to H_2O_2 and either 10 ppb C_{60} or 500 ppb $C_{60}(OH)_{24}$ for 48 hours. Both significantly increased mortality at 0.5 mM H_2O_2. Significance was determined using two-way ANOVA (*$p < 0.05$, $N = 24$). Error bars represent +/− the SEM.

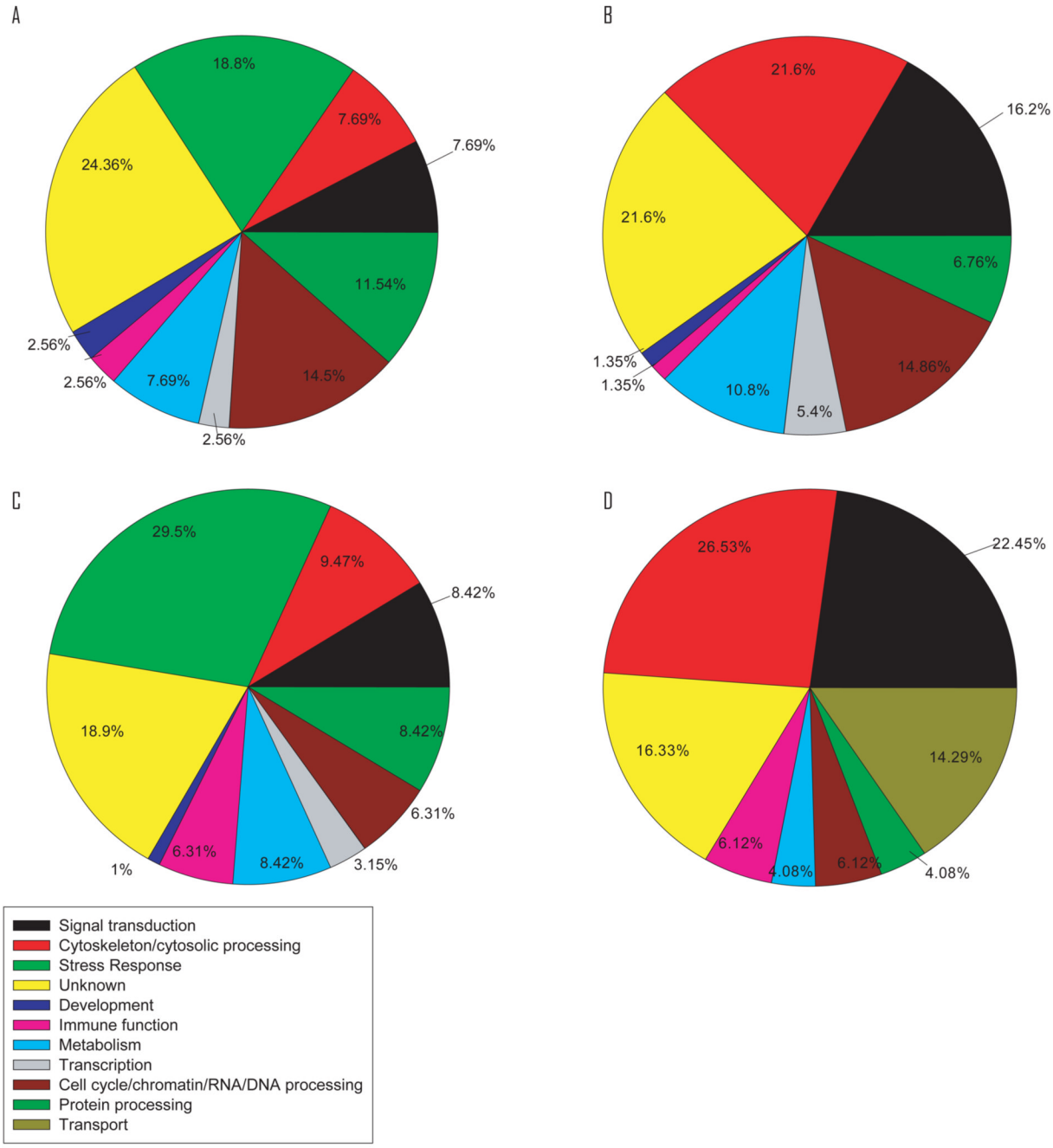

Figure 7. Pie chart of categories of gene regulation alterations

Differentially regulated genes were put into broad categories by stage and regulation: (A) 36 hpf up, (B) 36 hpf down, (C) 48 hpf up, (D) 48 hpf down. Stress response genes were only found to be up-regulated at both stages.

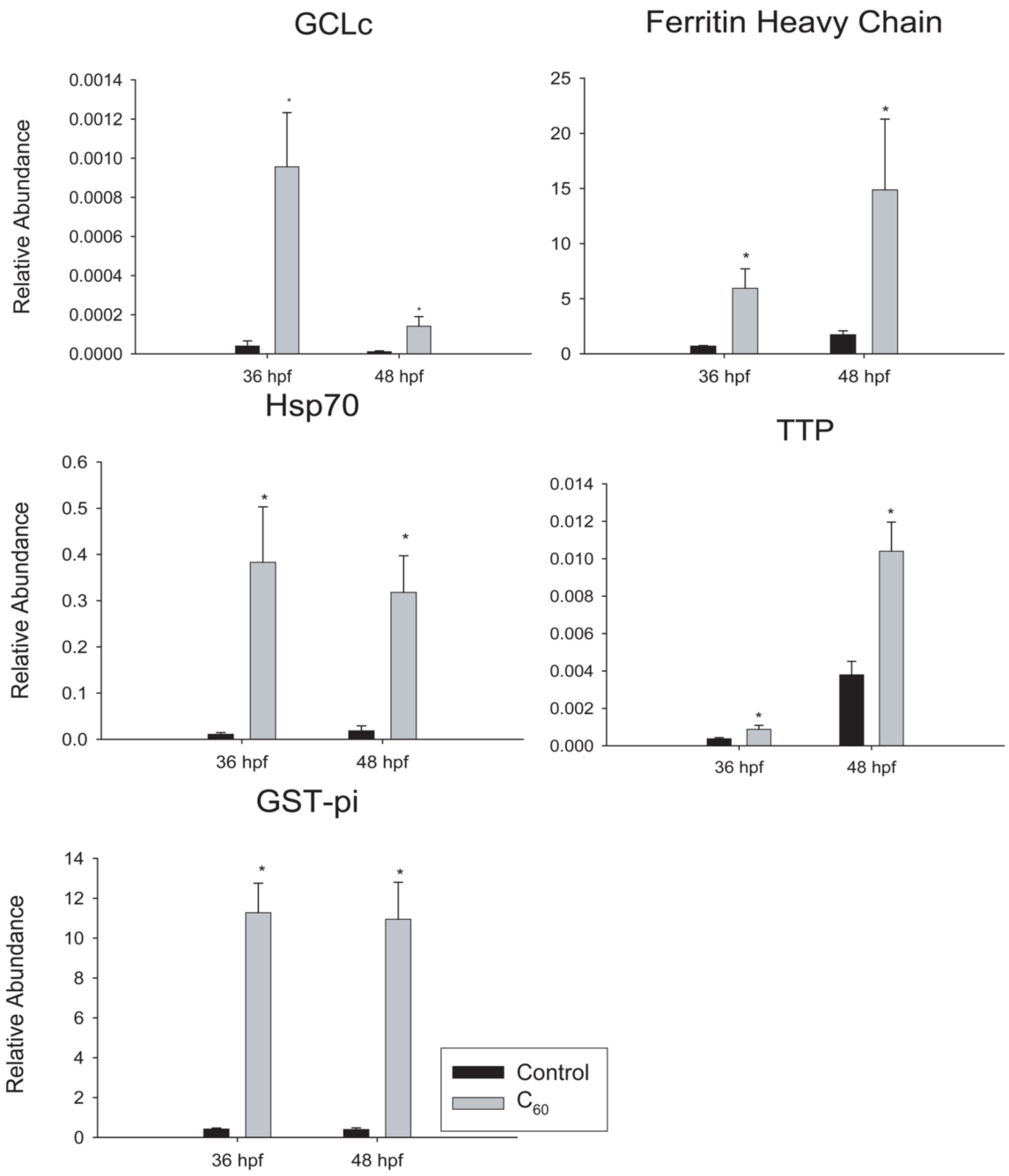

Figure 8. qRT-PCR results of gene expression

Genes involved in oxidative stress responses that were identified as mis-regulated by the microarray were further validated using qRT-PCR. Significance was determined using one-way ANOVA between controls and 200 ppb C_{60} treated (*$p < 0.05$, $N = 3$). Error bars represent the SEM.

Table 1

Primer sequences used in quantitative PCR. All products are between 180 and 300 mer.

Gene	Forward Primer	Reverse Primer
Ferritin heavy chain	5′-AGACACACTACTTGGACGAG	5′-AACAAGCTAGGAGGTTCTGC
HSP70	5′-GACCAAAGACAACAACCTGC	5′-ATGTTGAAGGCGTAAGACTCC
GCLc	5′-CTATCTGGAGAACATGGAGG	5′-CATTTTCCTCTGTTGACCGG
GAPDH	5′-GAATTCTGGGATACACGGAG	5′-AAAGGGGTCACATCTACTCC
GST-pi	5′-TTCAGTCCAACGCCATGC	5′-ATGAGATCTGATCGCCAACC
Tocopherol transport protein	5′-GTGTTTTGCTCATGCTCTGC	5′-ACTTCATCTACGCTGGGTCC

Table 2

Examples of misregulated genes. Several genes that were significantly up- or down-regulated at 36 hpf or 48 hpf compared to 1% DMSO controls were selected.

Reporter ID	Gene Name	36 hpf Average	36Standard Deviation	48 hpf Average	48 hpf Standard Deviation
Cell cycle/chromatin/RNA/DNA processing					
mwgzebrafish#04109	Biglycan-like protein 3	11.585	3.942	9.412	0.904
mwgzebrafish#05567	DCMP deaminase	5.986	1.124	3.403	1.000
mwgzebrafish#04079	Mob1/phocein	8.900	0.726	7.296	2.019
mwgzebrafish#04110	Wings apart	5.195	1.279	4.688	2.163
Cytoskeleton/Cytosolic Transport					
mwgzebrafish#05549	E-cadherin binding protein E7	10.391	3.233	5.756	1.575
mwgzebrafish#02873	Keratin 18	3.726	0.862	3.134	0.539
mwgzebrafish#06894	Beta-actin			0.280	0.023
Immune Function					
mwgzebrafish#04096	CTAGE family, member 5	4.665	0.864	3.875	0.448
mwgzebrafish#04064	Tec-family kinase	4.956	0.705	3.487	1.024
Metabolism					
mwgzebrafish#04095	Angiotensin converting enzyme	7.947	0.739	6.020	0.822
mwgzebrafish#00919	Cbr1l protein	8.035	1.971	5.063	0.540
mwgzebrafish#11641	Inosine triphosphate pyrophosphatase	5.625	3.587	2.715	0.156
mwgzebrafish#13913	Transketolase	3.112	0.280	3.040	0.350
Protein Processing/Degradation					
mwgzebrafish#12741	Cathepsin B	2.627	0.208	3.031	0.294
mwgzebrafish#04081	Esrom	8.228	0.201	7.710	2.500
mwgzebrafish#08710	Ubiquitin C	3.708	1.163	2.859	0.759
Signal Transduction					
mwgzebrafish#07570	CaM kinase	18.887	4.605	6.425	1.833
mwgzebrafish#01242	Neurogenin 1	10.825	4.724	5.662	0.877
mwgzebrafish#05534	RNA-binding region RNP-1	8.312	0.999	5.003	0.656
Stress Response					
mwgzebrafish#01262	Appb protein	6.920	0.908	5.730	0.667
mwgzebrafish#11036	Ferritin	15.994	1.393	7.482	1.976
mwgzebrafish#05998	Ferritin subunit 1	18.070	1.657	9.912	1.624
mwgzebrafish#00125	Glutathione S-transferase pi	11.527	1.276	9.723	0.781
mwgzebrafish#13567	Major vault protein	2.865	0.421	2.977	0.711
mwgzebrafish#08871	Sulfotransferase	4.616	0.953	3.931	1.624
mwgzebrafish#03954	Thioredoxin peroxidase	13.581	1.584	5.747	0.680
mwgzebrafish#00078	Hsp70	6.991	1.046	2.984	0.515
mwgzebrafish#07774	Glutamate-cysteine ligase, catalytic subunit alpha-tocopherol	4.926	0.677		
mwgzebrafish#05558	transfer protein	4.173	1.006		
mwgzebrafish#00120	Ferritin heavy chain	2.716	0.112	2.750	0.359